Optical responses through dilute anisotropic composites: Numerical calculations via Green's-function formalism

Y. Gu[1,2] and K. W. Yu[2]

[1] *State Key Laboratory for Mesoscopic Physics, Department of Physics, Peking University, Beijing 100871, China*

[2] *Department of Physics, The Chinese University of Hong Kong, Shatin, New Territories, Hong Kong, China*

Abstract

We investigate the linear and nonlinear optical responses of dilute anisotropic networks using the Green's-function formalism (GFF)[Gu Y et al. 1999 *Phys. Rev. B* **59** 12847]. For the different applied fields, numerical calculations indicate that a large third order nonlinear enhancement and a broad infrared absorption arise from the geometric anisotropy. It is also shown the overlap and separation between the absorption peak and nonlinear enhancement peak when the applied field is parallel, perpendicular to the anisotropy respectively. In terms of the inverse participation ratios (IPR) with $q = 2$ and spectral distribution of optical responses, the results can be understood.

PACC: 7430G, 8160H

I. INTRODUCTION

Recently, optical properties of composites have attracted great interest. In order to open new possibilities in the information processing and transmission, a large optical nonlinearity may be desirable [1]. Composite materials, especially, small metal particles embedded in a dielectric host and metal clusters on the nanometer scale, exhibit a strong nonlinear optical enhancement through the inhomogeneous local-field and geometric-response effect [1–4]. It is also known that these composites give rise to an anomalously large absorption in the infrared spectrum [5–7]. To analyze the optical responses, it is more convenient to adopt the spectral representation [8]. For various anisotropic composites, the spectral density was calculated as a function of volume fractions $p_{\|}$ and $p_{\perp}$ by the effective-medium approximation (EMA) [2,9,10]. It was found a large nonlinear optical enhancement, as well as the separation of the absorption peak from the nonlinear enhancement peak. By EMA, the fluctuation of local field has been averaged out. So it is difficult to find the physical origins of the optical enhancement and the separation of optical peaks. In this connection, Green's-function formalism (GFF) was developed to deal with the optical responses of the arbitrary-shaped metallic clusters embedded in the infinite dielectric networks at the quasistatic limit [11,12]. By the formalism, the resonance spectrum and local field distribution for each eigenmode can be analytically obtained. The aim of this paper is to investigate the linear and nonlinear optical responses throuth the dilute anisotropic networks in view of the local field distribution.

In the following, a binary dilute anisotropy network is considered. We use the random generator to produce the geometric anisotropy. The metallic bonds parallel to the applied field are assigned with the fraction $p_{\|}$, and metallic bonds perpendicular to the applied field with $p_{\perp}$. In the dilute systems, the condition, $p_{\|} \times p_{\perp} = 0.01$, is satisfied. When we change $p_{\|}$ from 0.1 to 0.8, the corresponding $p_{\perp}$ varies from 0.1 to 0.0125. In Section II, the Green's functions for the effective linear response ϵ_e and effective nonlinear response χ_e are derived. In Section III, the inverse participation ratios (IPR) with $q = 2$ are used to

represent the localized and extended eigenstates in anisotropic networks. In Section VI, the spectra of the absorption and the third order nonlinear enhancement are illustrated. When the applied field is parallel to the anisotropy of the networks, the overlap of the absorption peak with nonlinear enhancement peak is found within the interval $0.1 < p_{\|} < 0.8$. In contrast, for the perpendicular applied field, the separation of the absorption peak from nonlinear enhancement peak is enhanced when the anisotropy $p_{\|}$ is increased. These results are explained in Section III, numerically confirmed in Section VI, and concluded in Section V.

II. EFFECTIVE LINEAR AND NONLINEAR RESPONSES

Consider an infinite binary network as shown in Fig. 1, where the impurity bonds with admittance ϵ_1 are employed to replace the bonds in an otherwise homogeneous network of identical admittance ϵ_2. The admittance of each bond is generally complex and frequency-dependent. All the impurity bonds construct the clusters subspace. When resonance happens, the potential of the jointing points can be computed by the GFF. Instead of the point source $\delta_{\mathbf{x},\mathbf{0}}$[11], the source term is replaced by $\rho_{\mathbf{x}}$ at the point $\mathbf{x}$. Hence in the subspace, $\tilde{V}$ is a linear combination of right eigenvector $\tilde{R}$'s of Green's-matrix M,

$$\tilde{V} = \sum_{n=1}^{n_s} \frac{s}{\epsilon_2(s - s_n)} \sum_{\mathbf{y}\in\mathbf{C}} (\tilde{L}_{n,\mathbf{y}} \sum_{\mathbf{x}'} \rho_{\mathbf{x}'} \tilde{G}_{\mathbf{y},\mathbf{x}'}) \tilde{R}_n. \tag{1}$$

And for the site $\mathbf{x}(x_1, x_2)$ outside the cluster, $V_{\mathbf{x}}$ becomes

$$V_{\mathbf{x}} = \sum_{\mathbf{x}'} \rho_{\mathbf{x}'} \tilde{G}_{\mathbf{x},\mathbf{x}'} + \sum_{n=1}^{n_s} \frac{1}{\epsilon_2(s - s_n)} \sum_{\mathbf{y}\in\mathbf{C}} (\tilde{L}_{n,\mathbf{y}} \sum_{\mathbf{x}'} \rho_{\mathbf{x}'} \tilde{G}_{\mathbf{y},\mathbf{x}'}) \sum_{\mathbf{z}\in\mathbf{C}} M_{\mathbf{x},\mathbf{z}} \tilde{R}_{n,\mathbf{z}}. \tag{2}$$

FIGURES

FIG. 1. Schematic diagram of a cluster(shown in thick lines) embedded in an infinite network

In the uniform field E_0 along **1** direction, $\tilde{V}$ reads

$$\tilde{V} = \sum_{n=1}^{n_s} \frac{sE_0}{\epsilon_2(s-s_n)} (\sum_{\mathbf{y}\in\mathbf{C}} \tilde{L}_{n,\mathbf{y}} y_1) \tilde{R}_n. \tag{3}$$

For a binary network with $N \times N$ square lattices, in the quasistatic limit, the displacement $\mathbf{D}$ of the ith bond is related to the local field $\mathbf{E}$ by the relation $\mathbf{D} = \epsilon_\mathbf{i}\mathbf{E} + \chi_\mathbf{i}|\mathbf{E}|^\mathbf{2}\mathbf{E}$ [13], where ϵ_i is the dielectric constant and χ_i is the third order nonlinear susceptibility of the bond. ϵ_i, χ_i are set to be ϵ_1, χ_1 for the impurity bonds, and ϵ_2, χ_2 for the matrix bonds respectively. By the finite difference transformation, the effective linear response along the applied field is

$$\epsilon_e E_0 = \sum_{(\mathbf{x},\mathbf{y})\in\mathbf{C}} \frac{\epsilon_1(V_\mathbf{x} - V_\mathbf{y})}{a} + \sum_{(\mathbf{x}',\mathbf{y}')\notin\mathbf{C}} \frac{\epsilon_2(V_{\mathbf{x}'} - V_{\mathbf{y}'})}{a} \tag{4}$$

with the magnitude of field $E_0 = 1$ and lattice constant $a = 1$, where $(\mathbf{x},\mathbf{y}) \in \mathbf{C}$ means that $\mathbf{x}$ and $\mathbf{y}$ are the nearest neighbors in the same cluster while $(\mathbf{x}',\mathbf{y}') \notin \mathbf{C}$ means $\mathbf{x}'$ and $\mathbf{y}'$ are the nearest neighbors but not in the same cluster. When we employ $N(N+1)\epsilon_2 = \sum_{\mathbf{x},\mathbf{y}} \epsilon_2(V_\mathbf{x} - V_\mathbf{y})$, $\epsilon_2 - \epsilon_e$ can be expressed by the points within the clusters subspace as,

$$N(N+1)\epsilon_2 - \epsilon_e = \sum_{(\mathbf{x},\mathbf{y})\in\mathbf{C}} (\epsilon_2 - \epsilon_1)(V_\mathbf{x} - V_\mathbf{y}). \tag{5}$$

Here $\epsilon_1/\epsilon_2 = (s-1)/s$, so we have

$$N(N+1) - \frac{\epsilon_e}{\epsilon_2} = \sum_{n=1}^{n_s} \frac{1}{\epsilon_2(s-s_n)} (\sum_{\mathbf{y}\in\mathbf{C}} \tilde{L}_{n,\mathbf{y}} y_1) \sum_{(\mathbf{x},\mathbf{y})\in\mathbf{C}} (x_1 - y_1)(\tilde{R}_{n,\mathbf{x}} - \tilde{R}_{n,\mathbf{y}}). \tag{6}$$

Because $\mathbf{x}$ and $\mathbf{y}$ are neighbors, the values of $x_1 - y_1$ can be only $+1$ or -1. Physically, the absorption along the applied field is larger than that along the perpendicular direction of the applied field. In the following calculations, ϵ_e always represents the absorption along the applied field. For simplicity, we let $L_{\hat{n}} = \sum_{\mathbf{y}\in\mathbf{C}} \tilde{L}_{n,\mathbf{y}} y_1$, $R_{\hat{n}} = \sum_{\mathbf{x},\mathbf{y}\in\mathbf{C}} (x_1 - y_1)(\tilde{R}_{n,\mathbf{x}} - \tilde{R}_{n,\mathbf{y}})$, and $\gamma_n = L_{\hat{n}} R_{\hat{n}}$, the imaginary part of ϵ_e corresponding to the absorption is

$$-Im(\epsilon_e) = Im\sum_{n=1}^{n_s}\frac{\gamma_n}{\epsilon_2(s-s_n)}. \tag{7}$$

γ_n, referred to as the cross section, obeys the sum rule [14],

$$\sum_n \gamma_n = N_h \tag{8}$$

where N_h is the number of horizontal bonds along the applied field.

Since the local fields are determined completely, our formulas can be used to calculate the nonlinear response. By relating the total electrostatic energy to the effective coefficients, the third order nonlinearity χ_e' is defined by [13]

$$\int_v \mathbf{D}(\mathbf{x})\dot{\mathbf{E}}(\mathbf{x}) = V[\epsilon_e'\bar{\mathbf{E}}^2 + \chi_e'\bar{\mathbf{E}}^4], \tag{9}$$

where $\bar{\mathbf{E}} = (1/V)\int_v \mathbf{E}(\mathbf{x})\mathbf{d^3x}$ is the space averaged electric field. For the infinite networks, $\bar{\mathbf{E}} = \mathbf{E_0} = \mathbf{1}$ and the nonlinear response function is given by [9].

$$\chi_e' = \frac{1}{l^2}\sum_i \chi_i|\delta v_i|^2{\delta v_i}^2, \tag{10}$$

where the summation is over all bonds and δv_i is the(general complex) potential difference across the bond i and for two dimensional case, $V = l^2$. When all the bonds have nonlinear term, i.e., $\chi_1 = \chi_2 = 1.0$, with the lattice constant $a = 1$, the effective nonlinear response is written as

$$\chi_e = V\chi_e' = \sum_{(\mathbf{x},\mathbf{y})}|V_\mathbf{x} - V_\mathbf{y}|^2(V_\mathbf{x} - V_\mathbf{y})^2. \tag{11}$$

The third order nonlinearity χ_e is expressed as the summation of the forth moment of local electric field. So the fluctuation of local electric field enhances the nonlinear optical responses well.

III. INVERSE PARTICIPATION RATIOS WITH $Q = 2$

First, the IPR of eigenvectors of Green's-matrix M in the eigensystem with n_s jointing points are defined. The nth normalized right eigenvector is

$$R_n = \{R_{n,1},\ \ldots,\ R_{n,i},\ \ldots R_{n,n_s}\} \tag{12}$$

with $< R_n >= 0$ and $< {R_n}^2 >= 1$. The IPR of R_n is written as [15],

$$\mathrm{IPR}(R_n) = \sum_{i=1}^{n_s} {R_{n,i}}^{2q}. \tag{13}$$

Here $q = 2$. The calculation of $\mathrm{IPR}(R_n)$ is limited in the nontrivial eigenstates. The number of $\mathrm{IPR}(R_n)$ is equal to or less than n_s. In the above Eqs. (1) and (2), it is found that the right eigenvectors of M are closely related to the local fields of the impurity cluster in the subspace. So the IPR can be used to represent the localization of the eigenstates. The IPR amplify the profiles of eigenstates, namely, the localized states become more pronounced and extended states become smoother. Hence, the larger values of IPR are always corresponding to the stronger optical responses. This will be verified in the following sections.

To consider the size effect, the IPR in the dilute isotropic composites with $p_{\|} = 0.1$ and $p_{\perp} = 0.1$ are shown in Fig. 2. In this figure, two samples are in size 30×30 and 60×60. The peaks represent the localized states and the valleys correspond to the extended states. Comparing the distribution of peaks and valleys in two samples, we find that the size effect is not very obvious. It is also seen that the density of states are larger around $s = 0.5$ than that around $s = 0.0$ or $s = 1.0$. The localized states incline to accumulate $s = 0.0$ or $s = 1.0$, while, the extended states are near $s = 0.5$. So there exists a duality about $s = 0.5$ [12]. The high values of IPR imply the strong optical responses at $s = 0.0$ or $s = 1.0$.

FIG. 2. Size effect of IPR of right eigenvectors for two samples: 30×30 and 60×60. Here $p_{\|} = p_1 = 0.\ 1,\ p_{\perp} = p_2 = 0.\ 1$.

Fig. 3 displays the IPR of the dilute anisotropic systems. We have known that the resonance spectrum is very sensitive to the microstructure [12]. For each case, comparing two samples, we see that the peaks of IPR are very stable though their microstructure is completely different. So in the following, for the definite parameters $p_{\|}$ and $p_{\perp}$, it is

reasonable to investigate the optical responses by only one sample. When the anisotropy is increased from Fig. 3(a) to Fig. 3(g), the localized states incline towards $s = 0.\ 0$ or $s = 1.\ 0$. The distributions of localized and extended states have roughly the same feature as that in the isotropic case, i.e., we find more localized states at $s = 0.0$ and $s = 1.0$ than at $s = 0.5$, but denser at $s = 0.5$. The distribution of IPR is caused purely by the morphology of the sample. In the next section, we will discuss how the different applied fields act on the optical responses when the geometric anisotropy is increased.

FIG. 3. IPR of right eigenvectors of the dilute anisotropic systems. Sample 1 and sample 2 are randomly chosen. In (a) and (b), $p_{\|} = p_1 = 0.\ 2,\ p_{\perp} = p_2 = 0.\ 05$. In (c) and (d), $p_{\|} = p_1 = 0.\ 4,\ p_{\perp} = p_2 = 0.\ 025$. In (e) and (f), $p_{\|} = p_1 = 0.\ 5,\ p_{\perp} = p_2 = 0.\ 02$. In (g) and (h), $p_{\|} = p_1 = 0.\ 8,\ p_{\perp} = p_2 = 0.\ 0125$.

IV. SPECTRA OF ABSORPTION AND THIRD ORDER NONLINEAR ENHANCEMENT

The optical responses can be properly described by the absorption spectrum γ_n and the third order nonlinear enhancement spectrum as shown in Fig. 4 and Fig. 5. When the applied field is parallel to the direction of anisotropy, it affects the optical properties well. The envelopes of the absorption and third order nonlinear enhancements become narrower and the intensity is more enhanced with the increasing anisotropy. The main optical peaks are ranged in the interval $s \in [0.5, 0.6]$, which correspond to the dipolar approximation. In this figure, we can not find the separation of the absorption peak from the third order nonlinear enhancement peak. The results of single sample conflict with those of previous works [12]. The reason is that the EMA has averaged out the fluctuation of local field, which plays the central role for the effective optical responses. At $s = 0.5$, the density of localized states are much smaller than that of extended states. The optical properties of the specific sample are determined by its own eigenstates, not by "effective medium". So it

is not reasonable for all of the cases to express the optical properties of one specific sample only by the same macroscopic parameters $p_{\|}$ and $p_{\perp}$. In Fig. 5, when the applied field is perpendicular to the anisotropy, the optical responses of the dilute anisotropic samples are plotted. It is seen that the peaks of absorption are red-shifted while the peaks of the third order nonlinear enhancement are blue-shifted when the anisotropy is added. There is a larger peak separation with increasing geometric anisotropy. For all the applied fields, it is natural to find a large third order nonlinear enhancement and a broad infared absorption because the localized states exist in the whole resonant area. Only for the perpendicular applied field, the separation of optical peaks is found.

FIG. 4. Spectra of the absorption and the third order nonlinear enhancement of the dilute anisotropic systems for the parallel applied field. In (a) and (b), $p_{\|} = p_1 = 0.\ 2,\ p_{\perp} = p_2 = 0.\ 05$. In (c) and (d), $p_{\|} = p_1 = 0.\ 4,\ p_{\perp} = p_2 = 0.\ 025$. In (e) and (f), $p_{\|} = p_1 = 0.\ 5,\ p_{\perp} = p_2 = 0.\ 02$. In (g) and (h), $p_{\|} = p_1 = 0.\ 8,\ p_{\perp} = p_2 = 0.\ 0125$.

FIG. 5. Spectra of the absorption and the third order nonlinear enhancement of the dilute anisotropic systems for the perpendicular applied field. In (a) and (b), $p_{\|} = p_1 = 0.\ 2,\ p_{\perp} = p_2 = 0.\ 05$. In (c) and (d), $p_{\|} = p_1 = 0.\ 4,\ p_{\perp} = p_2 = 0.\ 025$. In (e) and (f), $p_{\|} = p_1 = 0.\ 5,\ p_{\perp} = p_2 = 0.\ 02$. In (g) and (h), $p_{\|} = p_1 = 0.\ 8,\ p_{\perp} = p_2 = 0.\ 0125$.

Then, the Drude free electronic model is employed to calculate the optical properties of the dilute anisotropic composites. The admittance of the impurity metallic bonds is

$$\epsilon_1 = 1 - \frac{\omega_p^2}{\omega(\omega + i\gamma)}, \tag{14}$$

where ω is the plasma frequency, and γ a damping constant. For metal, the plasma frequency ω_p 10^{16}, being in the ultraviolet. We choose $\gamma = 0.1\omega_p$, which is the typical value of a metal, and $\epsilon_2 = 1.77$, which is the dielectric constant of water for model calculations. The range of optical responses is $\omega/\omega_p \in (0, 1)$.

Optical responses of various anisotropic networks are illustrated in Fig. 6. The nonlinear enhancement $\chi^{(3)}$(or χ_e) is divided by 100 for the comparison with the linear absorption. The direction of anisotropy in Figs. 6(a), (c), (e) and (g) is parallel to the applied field. The peak at $\omega/\omega_p = 0.6$ corresponds to the dipolar approximation of the whole system. In these figures, the separation of absorption peak and nonlinear enhancement peak is not found, as observed in the above Fig. 4. Note that this result is different from that of the previous works [2,9,10]. However, when the applied field is perpendicular to the anisotropy, as shown in Fig. 6(b), (d), (f) and (h), in each of which, both the separation of linear and nonlinear peaks, and the third order nonlinear enhancement are seen.

FIG. 6. Linear and nonlinear optical responses of the dilute anisotropic systems by Drude model. Para.field means that the applied field is parallel to the anisotropy while perp.field is that the applied field is perpendicular to the anisotropy. Here p_1 is corresponding to $p_{\|}$ in the text and p_2 is $p_{\perp}$.

V. DISCUSSION AND CONCLUSIONS

In this paper, optical responses of dilute binary anisotropic networks are investigated numerically by the GFF. Green's functions for the effective linear and nonlinear responses are derived. The IPR with $q = 2$ are given to describe the localization and extension of eigenstates. The spectra of the absorption and the third order nonlinear enhancement are exhibited for the different applied fields. We also compute the optical responses for the Drude model. For the dilute anisotropic networks, we conclude that:

1. The size effect of optical responses is not obvious.

2. The IPR with $q = 2$ can be used to represent the localization and extension of eigenstates.

3. The wide optical absorption and large nonlinear enhancement are caused by the geometric anisotropy.

4. The peaks of the absorption and nonlinear enhancement overlap when the applied field is parallel to the anisotropy. While, for the perpendicular applied field, the absorption peak is separated from the nonlinear enhancement peak.

5. The structure sensitivity does not affect the main optical properties, but the details of optical responses.

¿From above 2, 3, 4 and the previous works [2,9,10], geometric anisotropy is the main reason to enhance the optical responses. For a specific sample, when the different fields are applied, the positions of optical responses do not vary, but the local field distributions are quite different. Therefore the optical properties of resonant composites are determined by the geometric anisotropy, as well as by the applied sources.

ACKNOWLEDGEMENTS

Gu Y acknowledges the useful discussions with Prof. Yang Zhan Ru.

REFERENCES

[1] See articles in: Bowden C M and Haus J W (ed) *J. Opt. Soc. Am. B* **6** (a special issue on nonlinear-optical properties of materials).

[2] Yuen K P, Law M F, Yu K W and Sheng P 1997 *Phys. Rev. E* **56** R1322.

[3] See articles in: Shalave V M 1997 *Nanostructured Materials: Clusters, Composites and Thin Films, ACS Symposium Series* **679** (American Chemical Society).

[4] Siu W H and Yu K W 1996 *Phys. Rev. B* **53** 9277.

[5] Tanner D B, Sievers A J and Buhrman R A 1975 *Phys. Rev. B* **11** 1330.

[6] Granqvist C G, Buhrman R A, Wyns J and Sievers A J 1976 *Phys. Rev. Lett.* **37** 625.

[7] Devaty R P and Sievers A J 1984 *Phys. Rev. Lett.* **52** 1344.

[8] Bergman D J and Stroud D 1992 *Solid State phyics* **146** 147.

[9] Law M F, Gu Y and Yu K W 1998 *Phys. Rev. B* **58** 12536.

[10] Law M F, Gu Y and Yu K W 1998 *J. Phys. : Condens. Matter* **10** 9549.

[11] Gu Y, Yu K W and Sun H 1999 *Phys. Rev. B* **59** 12847.

[12] Gu Y 2001 *PH.D Thesis*, copyrighted by the Chinese University of Hong Kong (CUHK).

[13] Yu K W, Hui P M and Stroud D 1993 *Phys. Rev. B* **47** 4150.

[14] Clerc J P, Giraud G, Luck J M and Robin Th 1996 *J. Phys. A: Math. Gen.* **29** 4781.

[15] Wegner F 1980 *Z. Phys. B* **36** 209.

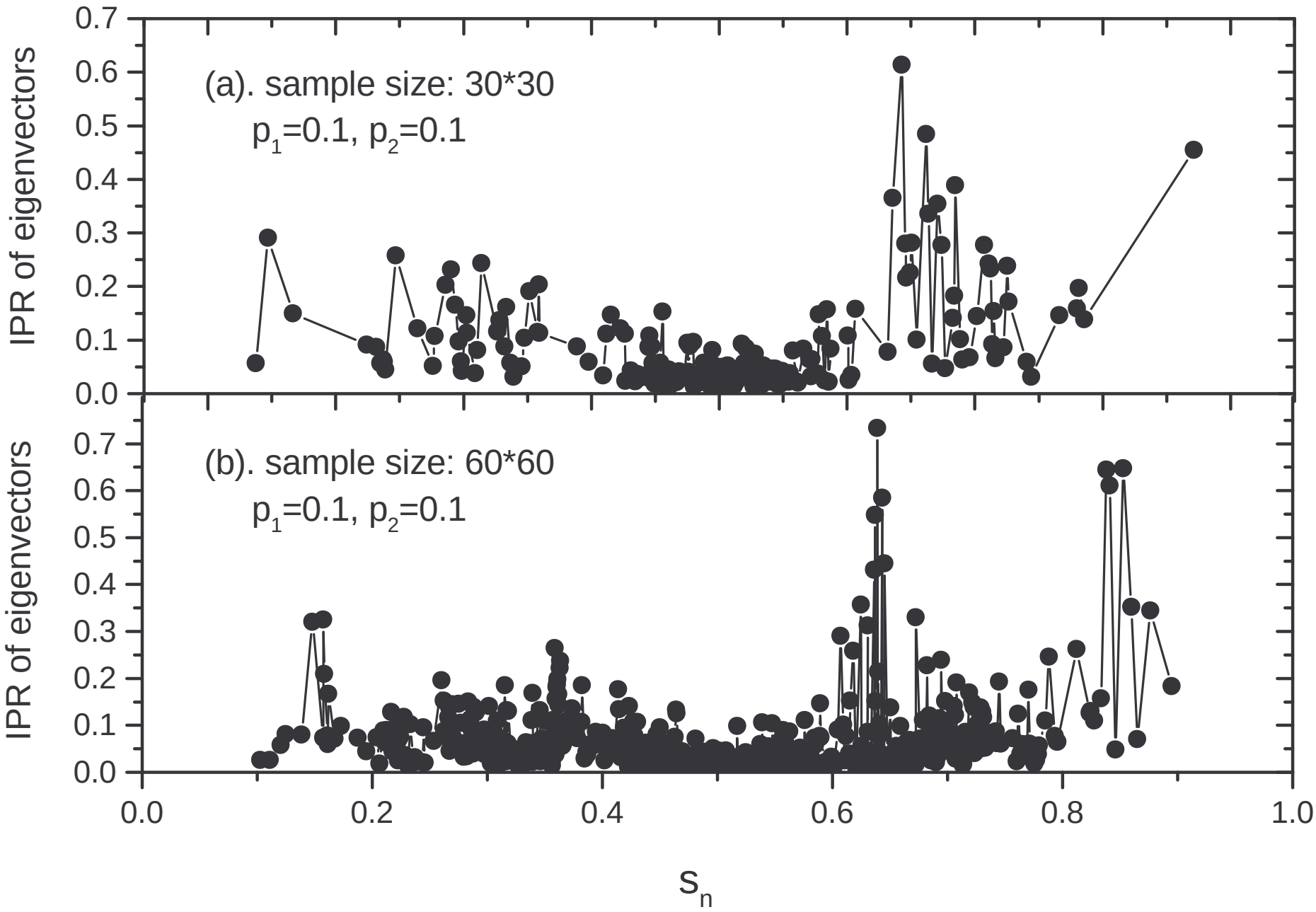
(a). sample size: 30*30
p_1=0.1, p_2=0.1
(b). sample size: 60*60
p_1=0.1, p_2=0.1
IPR of eigenvectors
IPR of eigenvectors
S_n
0.0
0.1
0.2
0.3
0.4
0.5
0.6
0.7
0.8
1.0

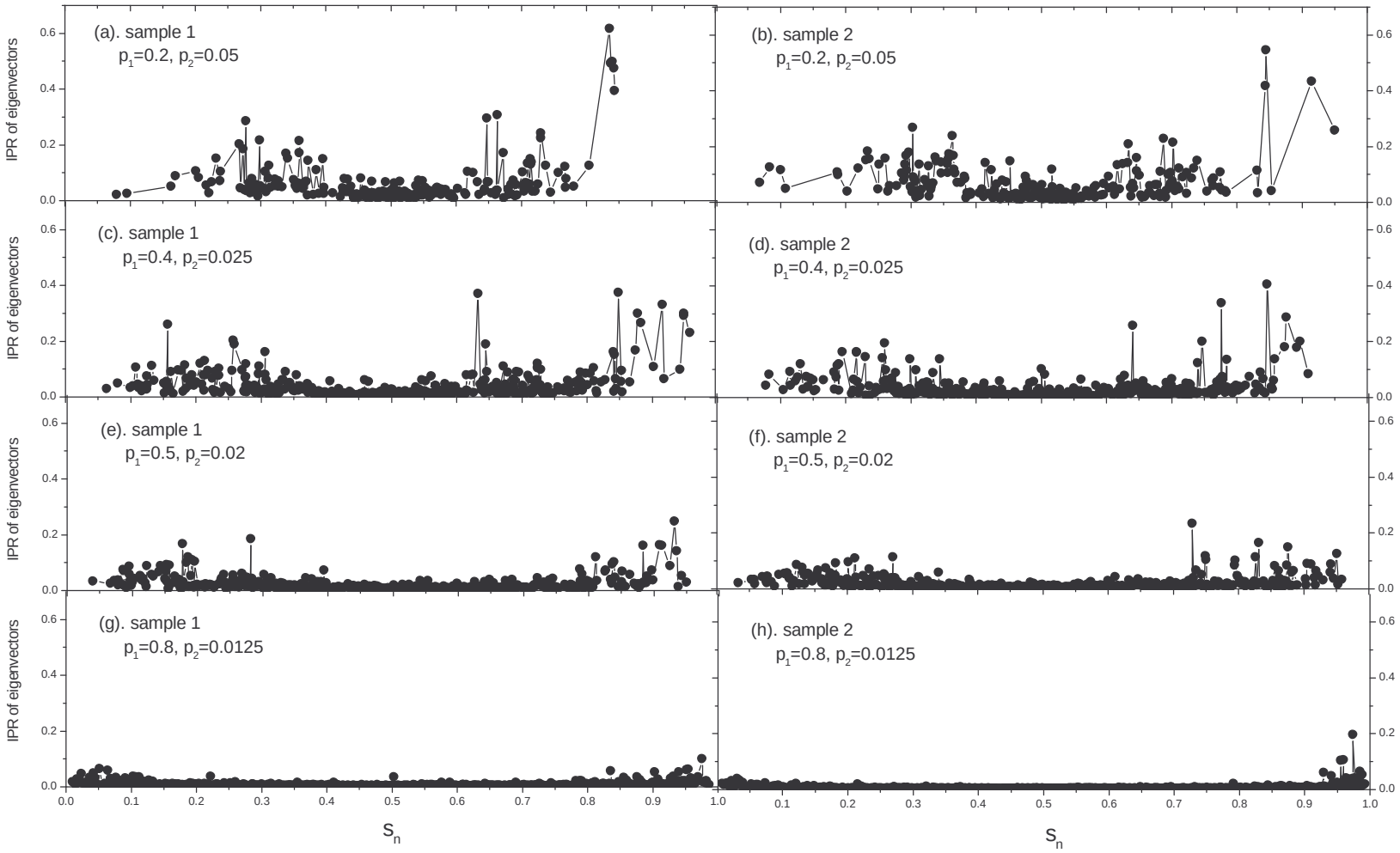
(a). sample 1
p1=0.2, p2=0.05
(b). sample 2
p1=0.2, p2=0.05
(c). sample 1
p1=0.4, p2=0.025
(d). sample 2
p1=0.4, p2=0.025
(e). sample 1
p1=0.5, p2=0.02
(f). sample 2
p1=0.5, p2=0.02
(g). sample 1
p1=0.8, p2=0.0125
(h). sample 2
p1=0.8, p2=0.0125
IPR of eigenvectors
Sn

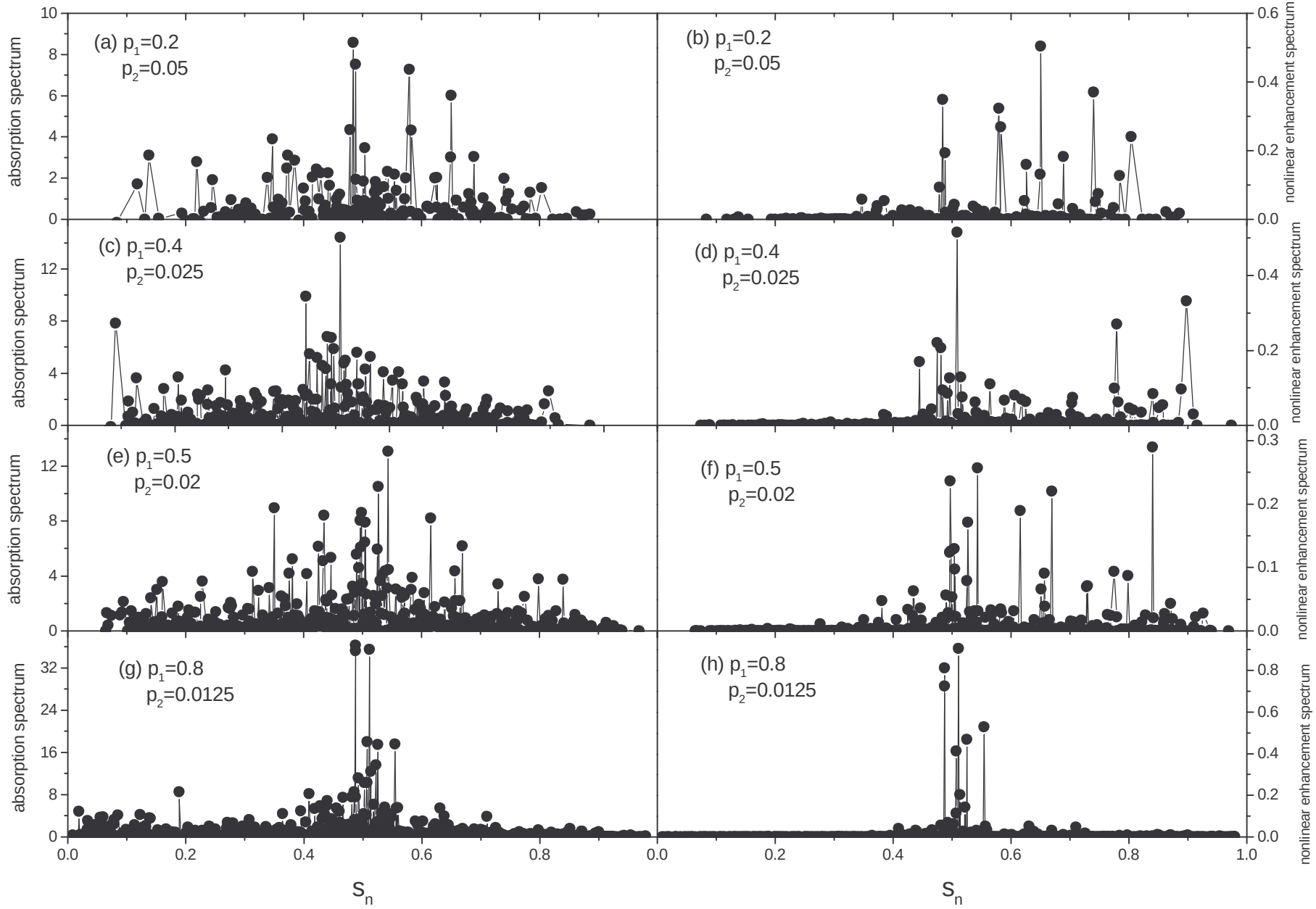
(a) p1=0.2
p2=0.05
(b) p1=0.2
p2=0.05
(c) p1=0.4
p2=0.025
(d) p1=0.4
p2=0.025
(e) p1=0.5
p2=0.02
(f) p1=0.5
p2=0.02
(g) p1=0.8
p2=0.0125
(h) p1=0.8
p2=0.0125
absorption spectrum
nonlinear enhancement spectrum
Sn

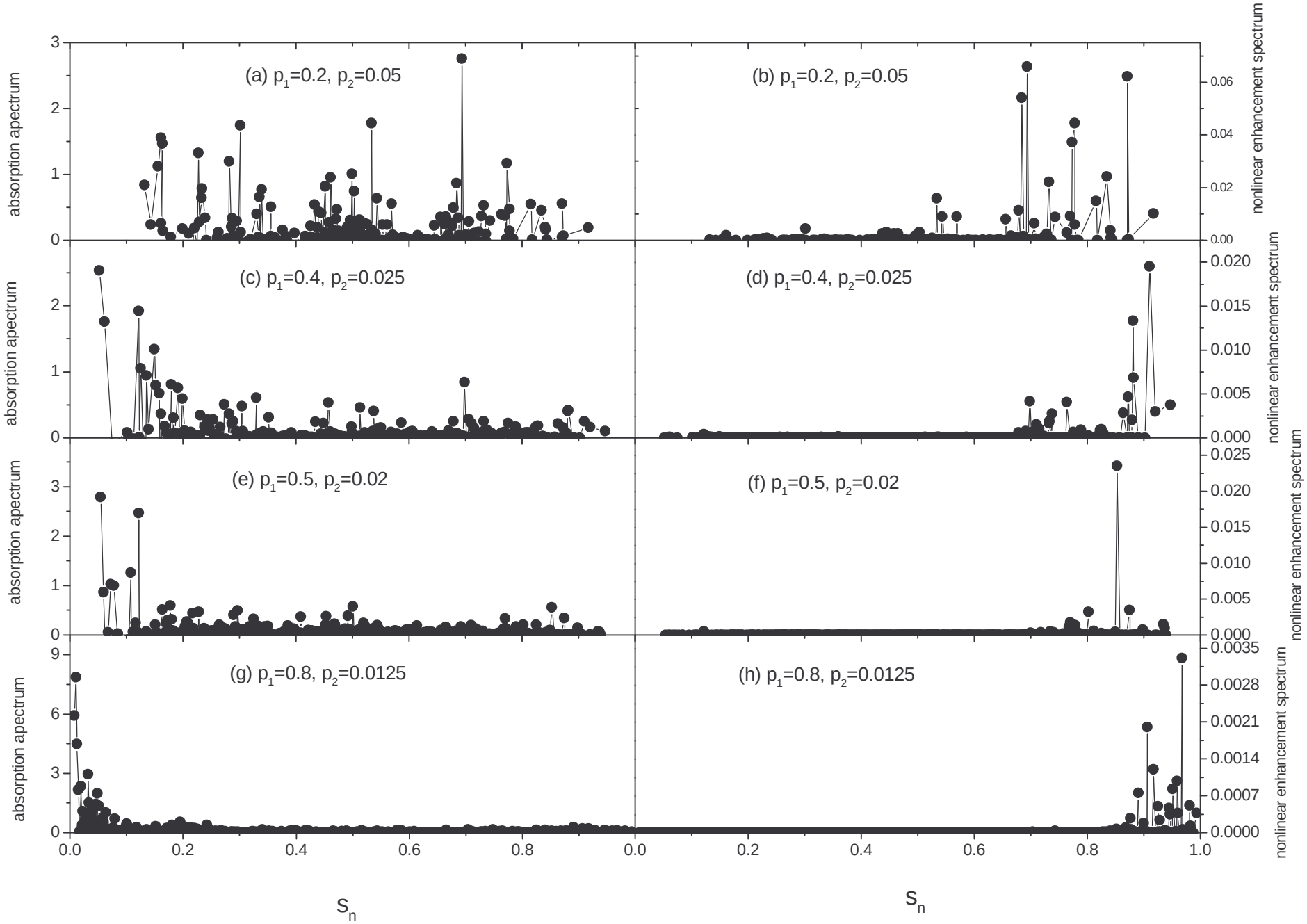
(a) p_1=0.2, p_2=0.05
(b) p_1=0.2, p_2=0.05
(c) p_1=0.4, p_2=0.025
(d) p_1=0.4, p_2=0.025
(e) p_1=0.5, p_2=0.02
(f) p_1=0.5, p_2=0.02
(g) p_1=0.8, p_2=0.0125
(h) p_1=0.8, p_2=0.0125
absorption apectrum
nonlinear enhancement spectrum
S_n

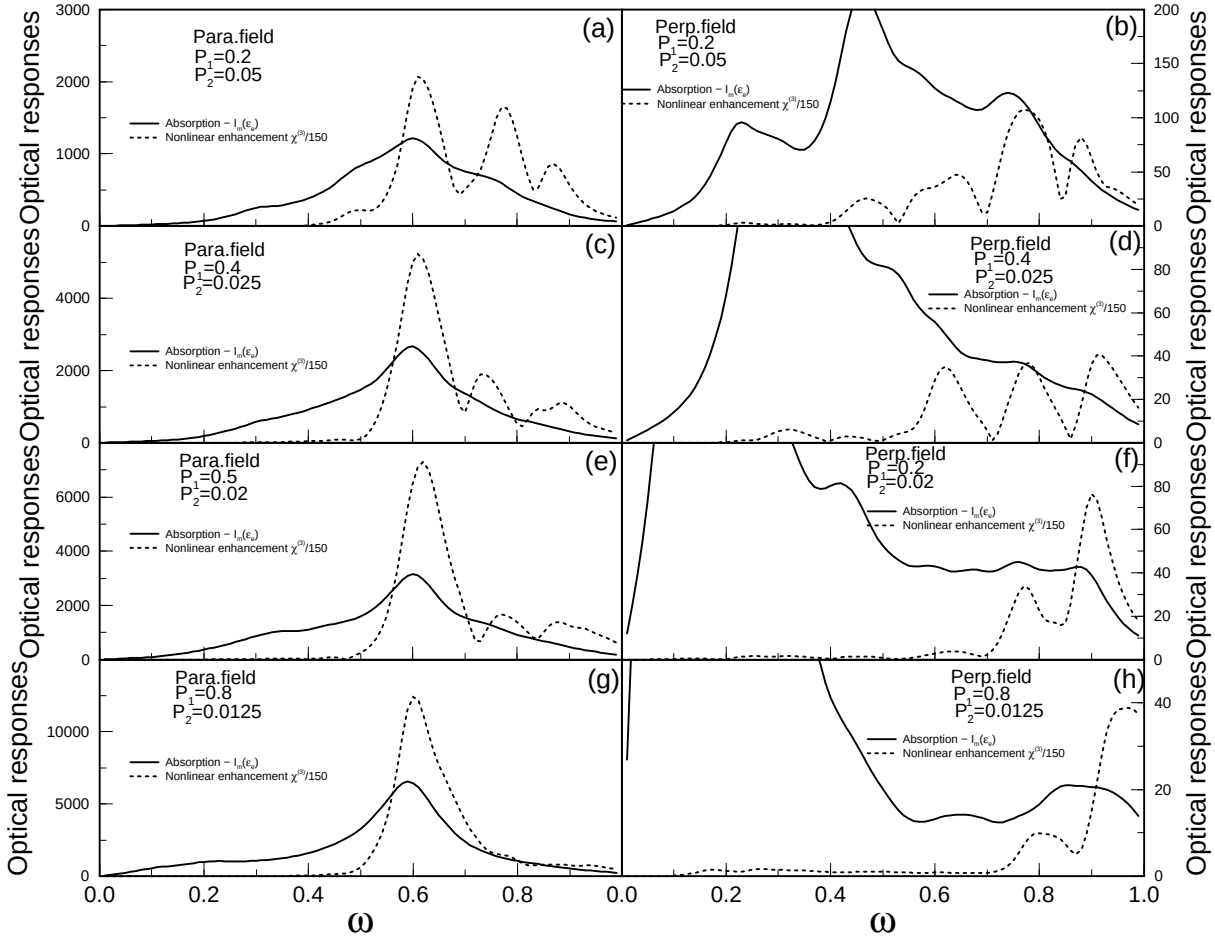
(a)
Para.field
P$_1^1$=0.2
P$_2^1$=0.05
(b)
Perp.field
P$_1^1$=0.2
P$_2^1$=0.05
(c)
Para.field
P$_1^1$=0.4
P$_2^1$=0.025
(d)
Perp.field
P$_1^1$=0.4
P$_2^1$=0.025
(e)
Para.field
P$_1^1$=0.5
P$_2^1$=0.02
(f)
Perp.field
P$_1^1$=0.5
P$_2^1$=0.02
(g)
Para.field
P$_1^1$=0.8
P$_2^1$=0.0125
(h)
Perp.field
P$_1^1$=0.8
P$_2^1$=0.0125
Absorption – Im(εω)
Nonlinear enhancement χ(3)/150
Optical responses
ω

Fig.2